地震波により励起された電磁波の地上への放射と地震発生前後の電磁波の波形

筒井 稔 [1]
[1] 京産大・コンピュータ理工

Waveforms of electromagnetic waves excited by earthquakes and radiated from teh ground surface

Minoru Tsutsui[1]
[1] Computer sciences, Kyoto Sangyo Univ

In order to detect electromagnetic (EM) waves which might be related to earthquakes, we had been observing EM noises in boreholes and above the ground. Although, in the observation, we had detected tremendous number of EM pulses with duration of a few millisecond in a frequency range of a few kHz, we could not detect any earthquake-related EM pulse at all. Almost all of the EM pulses were lightning and artificial ones. The reason why earthquake-related EM pulses could not be detected in the earth was considered as follows: the amplitude of the excited EM pulses could be strongly decayed during their propagations in the earth before its arrival at the EM observation site, because the earth's medium has electrically high conductivity. So we shifted down the monitoring frequency, from a few kHz to a few tens of Hz. As the result, we detected earthquake-excited EM pulses in the earth. During the period from December 2011 to March 2013, we confirmed thirteen earthquakes which excited EM pulses. From relations between magnitudes of these earthquakes and distances between epicentres and the EM observation site, we found that the EM waves were excited by seismic waves arrived near the EM observation site, due to Piezo-electric effect in the earth's crust.

From March 2013, we began simultaneous observations of EM waves by sensors in the borehole and above the ground, and the acceleration of seismic waves. At 05:33:17.7 JST April 13, 2013, we had a big earthquake (M6.3) in Awaji-shima island. The earthquake epicentre was about 115 km from the EM observation site. EM pulse was first detected by the sensor system installed above the ground at 05:33:40 JST, and 13.6 second later, a seismic wave was detected and its excited EM wave in the borehole. This result suggested that the EM wave excited by the seismic wave can readily leak out of the ground surface. These behaviours of earthquake-excited EM waves were published it in a paper [1].

Since we could not detect any EM pulse at the rupture time of the earthquake shown above, we focused on waveforms at/before earthquake occurrences. Waveforms of anther seismic wave and of its excited EM waves were shown in the figure below. However, we cannot recognize any specific fluctuations around the official rupture time (06:20:19.1 JST, April 4, 2014) of the earthquake (M3.3). At the time of 4 second prior to the official rupture time, intense pulses were detected by both sensor systems above the ground and in the borehole, and specific fluctuations were followed for 8.75 second. If we could identify that the intense pulse was radiated from the earthquake epicentre, we could regard the EM pulse as a precursor of the earthquake. Now we are preparing the system which can point arrival directions of this kind of EM pulse.

[1] Minoru Tsutsui, Behaviors of electromagnetic waves Directly Excited by Earthquakes, IEEE Geoscience and Remote Sensing Letters, Vol. 11, No. 11, pp. 1961-1965, 2014. (DOI: 1109/LGRS.2014.2315208, Now Open Access)

地震に伴って電磁波が励起されるだろうとの仮説の下、深さ 100 m の非導電性のボアホール内に電磁界センサーを挿入して、地中における電磁波の検出観測を行ってきた。　当初は数 kHz の周波数範囲での観測を行っていたが、検出されたのは雷放電に伴う電磁波のみで、地震に伴うものは全く検出されなかった。その理由は地中媒質の電気伝導度のため、励起された電磁波の地中伝搬中における減衰のためセンサーまでには到達しなかったと考えた。そこで観測する周波数を低くした結果、地震によって励起された電磁波を検出できるようになった。連続観測でそれを監視する方法は、一定時間幅毎に検出した信号を周波数分析し、その結果をディスプレイ上の縦軸を周波数とし、各周波数の強度を色で表し、順次同様の作業を繰り返えす事により、横軸に時間的に変化するスペクトログラムを用いた。

2011 年 12 月から 2013 年 3 月までの間に京都産業大学を中心とした領域で発生したマグニチュードが 2 以上の地震について調べたところ、19 件あり、そのうち 13 件についてはスペクトログラム上に現れ、地震に伴って発生した電磁波である事を確認した。これらの内、電磁波観測点に近い地震については、マグニチュードが小さい地震でも電磁波が検出され、遠方の地震の場合は、マグニチュードが大きければ遠方でも電磁波が検出された。この事は、電磁波観測点における地震波の強度により電磁波が励起されている事が考えられ、センサー近傍での岩盤の圧電効果によって励起された事を示唆している。このように地下岩盤で電磁波が励起されていることが明らかとなったので、その影響が地上にも現れている可能性を調べるため、地上にも同じ電磁波センサーを設置し、更にそれら電磁波と地震波との時間関係を明確にするために電磁波観測点にも地震波形を設置し、総合的な観測を開始した。

このシステムを用いての観測を続けていたところ、2013 年 4 月 13 日 05:33:17.7 JST に電磁波観測点の南西 115 km の淡路島の地下 14.8km で M6.3 の大地震が発生した。これによる電磁波をまず 05:33:40 JST に地上のセンサーで検出し、その 13.6 秒後に地震波形を検出し、それと同時にボアホール内で電磁波を検出した。この観測結果から、地震波による電磁波励起とその伝搬の様子が明らかとなった。即ち、岩盤内で地震波の波頭では常に電磁波を励起しており、それが

容易に地上へも放射している事を示している。これら地震波とそれによって励起された電磁波の伝搬について論文で発表した [1]。

上記のような結果を受けて、地震発生時あるいはそれ以前での電磁波励起について調査を開始した。2014 年 4 月 4 日 6:20:29.1 JST に電磁波観測点から西北西に 42.4km 離れた地点の深さ 10 km において地震 (M3.3) が発生した。この時の電磁波観測点において検出された各波形を図 1 に示す。地震波形は図の中央に、電磁波磁界の 3 軸方向成分の地上およびボアホール内で検出した波形をそれぞれ図中上半分及び下半分に示している。図から明らかなように電磁波観測点への地震波の到来（06:20:43.104 JST）時に地上では振幅の大きな電磁波を検出している。地震発生時刻（Official rupture time）(06:20:29.1 JST) での電磁波の波形には特別な変動は現れていない。しかし、その 4 秒前において地上および地中の両センサーで同時に急激なパルスが見られ、その後 8.75 秒間に極めて特徴的な振動波形が検出されている。この部分が震源で発生した事を確認できれば、地震発生前に励起された電磁波の一形態と見なす事が出来る。そこで今、この電磁波形の取得と同時に到来方位を測地出来るシステムの整備を進めている。

[1] Minoru Tsutsui, Behaviors of Electromagnetic waves Directly Excited by Earthquakes, IEEE Geoscience and Remote Sensing Letters, Vol. 11, No. 11, pp. 1961-1965, 2014. (DOI: 1109/LGRS.2014.2315208, Now Open Access)

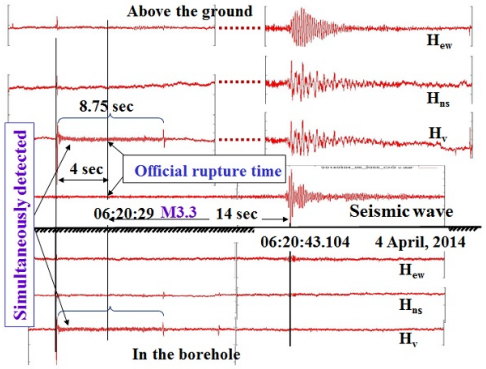

2011年東北地方太平洋沖地震における地震動・電離圏変動・津波起源の地電位差変動について

中谷 祐太 [1]; 中村 真帆 [2]; 長尾 年恭 [3]; 鴨川 仁 [4]
[1] 学芸大・F 類自然環境; [2] 東京学芸大・物理; [3] 東海大・海洋研・地震予知セ; [4] 東京学芸大・物理

Geoelectric potential changes caused by seismic waves, ionospheric disturbances, and tsunami

Yuta Nakatani[1]; Maho Nakamura[2]; Toshiyasu Nagao[3]; Masashi Kamogawa[4]
[1] Natural and Environmental Science, F, Gakugei Univ; [2] Physics, Tokyo Gakugei Univ.; [3] EPRC, IORD, Tokai Univ.; [4] Dept. of Phys., Tokyo Gakugei Univ.

We investigate geoelectric potential changes associated with the 2011 M9.0 off the Pacific coast of Tohoku Earthquake on long dipoles deployed at several stations in Izu Islands. The geoelectric potential changes originated from seismic waves, ionospheric E-region dynamo current due to acoustic waves excited by the tsunami and Rayleigh waves, tsunami dynamo and E-region dynamo currents due to other ionospheric disturbances, and electric field polarized by tsunami passing through the island were found. This result demonstrates that geo-electromagnetic changes associated with large earthquake and tsunami are detected by telluric current measurement with long dipoles.

伊豆諸島に複数配備されたキロメータースケールの長基線ダイポールを用いた地電位差観測データを用いて、2011年 M9.0 東北地方太平洋沖地震後の地電位差変動を調べた。その結果、次の４つの変動 (1) 地震動に伴う変動、(2) 津波ないしはレイリー波によって励起された音波が電離圏に到達することによって起きた E 領域ダイナモ電流起源の変動、(3) 津波ダイナモおよび電離圏の音波起源以外の変動、(4) 津波通過時に生じる孤島内分極による変動が検知された。以上の結果により、長基線地電位差観測によって地震後の津波および電離圏変動起源の地球電磁気的変動検知が可能であることが分かった。

海底電磁場データを用いた津波速度場の推定

川嶋 一生 [1]; 藤 浩明 [2]
[1] 京大・理・地惑; [2] 京都大学・大学院・理学・地磁気センター

Estimation of tsunami velocity field using seafloor electromagnetic data

Issei Kawashima[1]; Hiroaki Toh[2]
[1] SPEL, Kyoto Univ.; [2] DACGSM, Kyoto Univ.

A pair of earthquakes occurred on both sides of the Kuril Trench on 15 November 2006 and 13 January 2007. The interplate underthrust earthquake of the 2006 event (Mw 8.1) had a larger seismic moment than the outer-rise normal fault earthquake of the 2007 event (Mw 7.9) (Fujii and Satake, 2008). Toh et al. (2011) reported that the electromagnetic (EM) variations during the tsunami passages were recorded about 1 hour after the origin time of each earthquake by a seafloor geomagnetic observatory located about 800km away from the epicenters. The article also reported that the relationship between the EM variations and the particle motions of conductive seawater are confirmed using Sanford's (1971) theory.

However, Sanford's (1971) theory neglects the self-induction effect and is applicable only to ocean currents moving slowly. The phase velocity of tsunami in pelagic environments exceeds 200 m/s and hence the self-induction term needs to be considered. Here we report our simulation result on the tsunami-induced EM signals observed at the seafloor based on three-dimensional (3-D) non-uniform thin-sheet approximation by McKirdy, Weaver, and Dawson (1985). Our newly written numerical code accommodates not only the inducing non-uniform source fields caused by particle motions of conducting seawater at the time of tsunami passage but also the self-induction effect within the ocean and its conductive substrata. Horizontal particle motions were calculated by Fujii and Satake (2008) with two types of hydrodynamic approximation, viz the Boussinesq approximation and the long-wave approximation.

The calculated EM variations associated with the initial wave of the tsunami at the time of 2006 event are consistent with the observed ones even by the long-wave approximation, while the numerical predictions do not reproduce the observation associated with subsequent tsunami phases.

As for 2007 event, the EM variations accompanied by distinct subsequent tsunami phases are partly simulated by the Bousinessq approximation. However, the amplitudes of the calculated EM variations were about half of those of the observation in both hydrodynamic approximations used here.

The disagreement between the calculation and the observation probably stems from the assumed tsunami velocity field, for there were no tsunami waveform observatories near the seafloor geomagnetic observatory when the two tsunamis occurred.

We, therefore, estimate the tsunami waveforms that explain the observed EM variations. The waveforms are calculated by Cornell Multi-grid Coupled Tsunami Model (COMCOT, Version 1.7), which employs linear water equations and applies the method to mimic physical dispersion by numerical dispersion proposed by Imamura et al. (1988) to weak dispersive waves over slowly varying bathymetry. The EM observatory locates in the open ocean where the bathymetry slowly varies so that the dispersion effect of the tsunami was recovered in the case of 2006 event. As for the 2007 event, the dispersion effect was larger and hence this model was not sufficient to reproduce the dispersion of the latter event. This implies that seafloor EM data can be used to recover tsunami velocity fields at least for weakly dispersed tsunamis.

ベクトル津波計による微小津波の検出

浜野 洋三 [1]; 杉岡 裕子 [2]; 多田 訓子 [2]; 藤 浩明 [3]; 南 拓人 [4]
[1] JAMSTEC; [2] 海洋研究開発機構・IFREE; [3] 京都大学・大学院・理学・地磁気センター; [4] 京大・理・地物

Detection of micro-tsunamis by using Vector Tsunameter

Yozo Hamano[1]; Hiroko Sugioka[2]; Noriko Tada[2]; Hiroaki Toh[3]; Takuto Minami[4]
[1] JAMSTEC; [2] IFREE, JAMSTEC; [3] DACGSM, Kyoto Univ.; [4] Geophysics, Kyoto Univ.

We developed a new type of offshore tsunami meter called Vector TsunaMeter (VTM) for the purpose of providing early and reliable information on the generation and propagation of tsunamis in order to predict the tsunami impact at the coastal area. The VTM observes and records three components of the geomagnetic fields, two horizontal components of the electric fields and tilts, and a differential bottom pressure for more than a year at sea floor up to 6000 m of water depth. The VTM is designed to detect the temporal variations of sea level change, and particle motion associated with the tsunami passages. Arrival time, arrival direction, and phase velocity of tsunamis can also be calculated from the observed record of the VTM. These characteristics of tsunamis observed at deep ocean far from the coastline are very useful to forecast the arrival time and the size of tsunamis before the tsunami reaches the coastline. The first seafloor observation of VTM was made during 2012-2013, in which the VTM was installed by KR12-18 cruise of R/V KAIREI on November 20, 2012 at 25 45.94N, 137 00.48E, depth=4894m, and recovered during KR13-02 cruise on February 9, 2013. The VTM continuously record the data sets of, Bx, By, Bz, Ex, Ey, TiltX, TiltY, and Bottom Pressure from Nov. 20, 2012 to the recovery time, i.e. Feb. 9, 2013. Three days before the recovery date, a Mw=8.0 earthquake occurred at the Solomon islands (10.738S, 165.138E) on 2013-02-06 01:12:27UTC. The earthquake generated tsunamis, which hit near Solomon islands and caused damages to human beings and houses. Since the main energy of the tsunami propagates along the north-east to south-west direction from the epicenter of the earthquake, the tsunamis observed at Japanese coast were low. At the observational site of VTM, amplitude of the first wave is as small as 1 cm, but the VTM clearly records the variations of sea level change for more than several hours after the tsunami arrival around 2013-02-06 08:40 UTC. This observation indicates the resolution limit of VTM is less than 1 mm of sea level change.

The next seafloor measurement of VTM started on March 13, 2014, in which the VTM was installed during KS14-2 cruise of R/V Shinsei-maru. We installed the VTM on the seafloor at 38 14.0 N, 143 35.13 E, depth=3420.1 m, and, after the installation of VTM, we deployed the Wave Glider on the sea surface around the VTM site, and started real-time monitoring of the seafloor VTM signal right after the installation. During the real-time observation period, we succeeded in detecting the micro-tsunami from the Chile earthquake. The Chile tsunami was generated by the Mw=8.2 earthquake , occurred on 2014-04-01 23:46:46 UTC, at 95km (59mi) NW of Iquique, Chile (19.642 S 70.817 W) . The tsunami arrived at the VTM site in the early morning of April 3, 2014. Since the arrival of the tsunami was expected about a day beforehand, we could observe the tsunami with the VTM of tsunami mode, in which the tsunami signals with 10-second sampling interval was transferred to the land station every one minute. Although the tsunami signal at the VTM site is very small, and the amplitude of the first wave is as small as 0.1 cm, the arrival of tsunami was clearly detected by the DPG raw data at around 06:00 LT. After applying the high pass filter, the pressure variation faithfully reproduce the wave form of the tsunami. The amplitude of the tsunami signals in the north-south component of the electric field and the east-west component of the magnetic field is much higher than the other component, indicating the tsunami arrived form the east direction.

中央構造線断層帯（和泉山脈南縁－金剛山地東縁）の地殻比抵抗構造

吉村 令慧 [1]; 米田 格 [1]; 小川 康雄 [2]
[1] 京大・防災研; [2] 東工大・火山流体

Crustal resistivity structure around the Japan Median Tectonic Line Izumi-Kongo fault zone

Ryokei Yoshimura[1]; Itaru Yoneda[1]; Yasuo Ogawa[2]
[1] DPRI, Kyoto Univ.; [2] VFRC, Titech

The fault geometry, especially dip angle, and structural heterogeneity are important information for estimation of strong ground motion and evaluation of earthquake size. In order to pursue the sophistication of such estimation and evaluation for the Japan Median Tectonic Line Izumi-Kongo fault zone, we plan to carry out wideband magnetotelluric (MT) surveys along three profiles, two are across the Izumi segment and the other is across the Kongo segment. Along the previous seismic survey line (Sato et al, 2007), wideband MT measurements at 6 sites were performed in January, 2014. We calculated MT responses from hundreds to 0.1 Hz using only nocturnal data after remote referencing to the Esashi observatory (Geospatial Information Authority of Japan) and inverted the data in TM mode using 2D inversion code (Ogawa and Uchida, 1996). Our 2D resistivity model showed consistency with seismic reflectors (Sato et al, 2007) and north dipping structural tendencies from surface up to several kilometers depth. In this presentation, we will show the outlines of our research project and report the result of 2D inversions. Additionally, we will introduce new surveys now underway.

中央構造線断層帯の和泉山脈南縁－金剛山地東縁セグメントが活動した場合の強震動評価や破壊の規模の予測のためには、震源断層の形状の把握と地下の不均質構造の理解が重要となる。我々は、文部科学省「中央構造線断層帯（金剛山地東縁－和泉山脈南縁）における重点的な調査観測」の一環として、広帯域 MT 法探査を用いた地殻比抵抗構造の推定を行っている。

平成 25 年度に、ノイズ環境調査を念頭に 6 測点による広帯域 MT 観測を実施した。測点は、既存の反射法地震探査測線（佐藤他，2007）に沿う南北測線に設定している。各観測点で 10 日前後の電場 2 成分、磁場 3 成分の連続測定を行い、国土地理院江刺観測場の電磁場時系列データをリファレンス信号として MT 応答を推定した。昼間に比較して、人工電磁ノイズが低減する時間帯が夜間に 2 時間ほど確認でき、その時間帯のみ MT 応答の推定に用いている。結果として、数 100Hz～0.1Hz の帯域で良好なインピーダンスを得ることができ、Ogawa and Uchida （1996）の 2 次元構造解析プログラムを用いて逆解析を行った。得られた結果は、佐藤他（2007）の反射法地震探査から得られた反射層との明瞭な対応関係がみられ、その特徴は以下の通りである。（１）和泉山脈南縁セグメントの根来断層を横切るが、その地表位置から約 30 度で北傾斜する構造コントラストが確認できたものの、2km 以深では測線北部に位置する領家帯花崗岩に対応する高比抵抗にかかり追跡できない。（２）三波川帯は上面のみならず大局的に北傾斜の傾向が確認できるが、パッチ状の表層低抵抗体（菖蒲谷層に相当）により複雑な様相を示す。（３）三波川層の内部構造を示すとされる反射層群は、相対的な高比抵抗領域に集中している。（４）測線中央部の深部（3km 以深）に検出された低比抵抗体の上面は、浅部では 30 度程度で北傾斜し、深部に向かい高角に遷移する。

本発表では、平成 25 年度の観測概要ならびに 2 次元解析結果を報告するとともに、 現在実施中である和泉山脈南縁セグメントでの別測線（12 観測点）、金剛山地東縁セグメントを東西に横切る測線（12 観測点）での観測概要・予備的解析結果を紹介する予定である。

年代に伴う海洋マントル冷却モデルと北西太平洋の電気伝導度構造

馬場 聖至 [1]; 多田 訓子 [2]; 梁 朋飛 [1]; Zhang Luolei[3]; 清水 久芳 [4]; 歌田 久司 [3]
[1] 東大・地震研; [2] 海洋研究開発機構・IFREE; [3] 東大・地震研; [4] 東大・地震研

Age-dependent cooling model for oceanic mantle and electrical conductivity beneath the northwestern Pacific

Kiyoshi Baba[1]; Noriko Tada[2]; Pengfei Liang[1]; Luolei Zhang[3]; Hisayoshi Shimizu[4]; Hisashi Utada[3]
[1] ERI, Univ. of Tokyo; [2] IFREE, JAMSTEC; [3] ERI, Univ. Tokyo; [4] ERI, University of Tokyo

Oceanic upper mantle beneath the northwestern Pacific has large-scale lateral heterogeneity that is impossible to attribute to just an age-dependency of the thermal structure based on a cooling of homogeneous mantle with age. This surprising fact was revealed from seafloor magnetotelluric (MT) data collected in three areas, northwest (Area A) and southeast (Area B) of the Shatsky Rise, and off the Bonin Trench (Area C), through the Normal Oceanic Mantle Project and the Stagnant Slab Project. One-dimensional structures of electrical conductivity representing each area show significant difference in the thickness of the upper resistive layer that may be interpreted as cool lithosphere. The thickness of the layer that is more resistive than 0.01 S m^{-1} is about 80 km for Area A, about 110 km for Area B, and about 180 km for Area C. The conductivity below the resistive layer is similar to about 0.03 S m^{-1} for Areas A and C but a slightly higher than it for Area B. The thermal structures for the lithospheric age representing the areas (130, 140, and 147 Ma for Areas A, B, and C, respectively) predicted from a simple plate cooling model are almost identical and thus cannot reproduce such variations in electrical conductivity.

In this study, thermal and compositional states of the mantle beneath the three areas were investigated to discuss the cause of the variations. Combination of five model parameters, electrical conductivity of crust, mantle potential temperature, thickness of thermally conductive plate, and H_2O and CO_2 contents in the asthenospheric mantle were searched by forward modeling and the chi-squared misfit between the MT responses observed and predicted were assessed with 95% acceptable level. The possibility of partial melting was taken into account by comparing to the solidus of peridotite that is reduced by H_2O and CO_2. We assumed that the mantle conductivity may be represented by the mixture of hydrous olivine and hydrous carbonated melt. The results shows significant difference in the thickness of thermally conductive plate and CO_2 content among the three areas, suggesting a possible influence of a mantle up-welling associated with the formation of the Shatsky Rise to the mantle beneath Areas A and B although these areas are away from the bathymetric anomaly.

北西太平洋の上部マントルは大規模な横方向不均質構造をもち、それは一様なマントルの海洋底形成年代に伴う冷却モデルでは説明することができない。我々が数年来北西太平洋で行ってきた海底マグネトテルリック (MT) 探査は、このような驚くべき結果を示している。シャツキーライズの北西海域（A 海域）、南東海域（B 海域）、小笠原海溝沖太平洋海域（C 海域）において得られた平均的 1 次元上部マントル電気伝導度構造の間にはモデル推定誤差を考慮しても有意な差が見られる。低温のリソスフェアと一般に解釈される上部低電気伝導度 ($<$ 0.01 S m^{-1}) 層の厚さは、A 海域では約 80 km、B 海域では約 110 km、C 海域では約 180 km であり、その下の高電気伝導度領域は、A・C 海域では約 0.03 S m^{-1} であるが、B 海域では、それよりもやや高い。3 つの海域の海洋底生成年代は、それぞれ約 130、約 140、約 147 Ma であるが、一様なマントルの冷却モデルを考える限り、このような古い海洋マントルのわずかな年代差では温度構造に大きな差はなく、したがって電気伝導度構造に見られる差を再現できない。

本研究では、3 海域の間の電気伝導度構造の差を説明すべく、温度構造と組成の不均質性について以下のアプローチを試みた。電気伝導度を制約するモデルパラメータとして、海洋地殻の電気伝導度、マントルのポテンシャル温度、熱伝導層の厚さ、マントル中の水の量と二酸化炭素の量を考え、フォワードモデリングにより MT レスポンスを計算し、観測から得られた MT レスポンスとの間のカイ 2 乗ミスフィットを 5 %有意水準で評価する。温度構造は、プレート冷却モデルに基づき計算する。水と二酸化炭素量の効果を考慮したマントルペリドタイトのソリダス温度を計算し、温度構造がソリダス温度より高くなる深さでは部部分溶融を考慮する。マントルの電気伝導度は水を含むオリビンと水と二酸化炭素を含むメルトの混合で考える。この手法を 3 海域の MT レスポンスに適用した結果、熱伝導層の厚さが C 海域に比べて A・B 海域で薄く、二酸化炭素量が B 海域で特に多いことが有意であることが分かった。これらの差をつくる要因として、シャツキーライズの形成に寄与したマントル上昇流の影響が A・B 海域に及んでいる可能性が考えられる。

ガルバニックディストーションがある場合のMTインピーダンスの回転不変量

Rung-Arunwan Tawat[1]; Siripunvaraporn Weerachai[2]; # 歌田 久司 [3]
[1] Mahidol Univ., Thailand; [2] Mahidol University, Thailand; [3] 東大・地震研

Rotational invariants of the magnetotelluric impedance tensor with galvanic distortion

Tawat Rung-Arunwan[1]; Weerachai Siripunvaraporn[2]; # Hisashi Utada[3]
[1] Mahidol Univ., Thailand; [2] Mahidol University, Thailand; [3] ERI, Univ. Tokyo

As shown by Szarka and Menvielle (1997), a complex magnetotelluric (MT) impedance tensor having 4 independent complex elements (8 independent real elements) has 7 independent rotational invariants. For example, determinant invariant scalar impedance is most often used in MT studies both on land and at seafloor. Here we consider a case where impedance has galvanic distortion: i.e., there is distortion of the electric field due to near-surface, small-scale lateral heterogeneities of the electrical conductivity.

We apply a model of galvanic distortion proposed by Groom & Bailey (1989), in which distorted impedance tensor is expressed by a product of the site gain, three elementary real tensors (the twist, shear and anisotropy) and the regional (undistorted) impedance tensor. If we calculate the determinant invariant Zdet of distorted impedance, it is shown that amplitude (or apparent resistivity) of Zdet is biased downward by twist and shear. This property is inconvenient when we use the determinant invariants to estimate a regionally averaged (background) 1-D profile (e.g. Berdichevsky, 1980).

Recently we examined the behavior of another (less well-known) rotational invariant, the sum of squares (ssq) of impedance elements, ssq(Z) = Zxx^2+Zxy^2+Zyx^2+Zyy^2. The effective 1-D scalar impedance is derived as, Zssq = [ssq(Z)/2]^(1/2). Then we found that Zssq is not biased by distortions (shear, and anisotropy) but only by site gain (static shift). This means that, if we have many MT measurements in a region, a reasonable estimation of regional 1-D background model can be obtained by inverting averaged Zssq (not Zdet) over all stations. Such a 1-D model is convenient for various aspects of MT analyses as a good starting and/or a priori model.

Another finding is that the ratio of corresponding apparent resistivities (rho-ssq/rho-det) will always be greater than unity under the presence of galvanic distortion. If the regional structure is 1-D, the ratio Zssq/Zdet will be a real number (phase=0), otherwise it will be a complex number. Thus these quantities (ratio and phase) can be used as an indicator for the presence of galvanic distortion and 3-dimensionality of regional structure, which tells us the right treatment of a given dataset.

Three-dimensional inversion of magnetotelluric data using unstructured tetrahedral elements

Yoshiya Usui[1]
[1] Earth and Planetary sciences, Tokyo Tech.

3-D magnetotelluric inversion code using unstructured tetrahedral elements is newly developed in order to correct topographic effect by directly incorporating it in computational grid. Electromagnetic field and response functions are distorted at the observing sites of magnetotelluric (MT) method due to undulating land surface. Without correcting the distortion, we can wrongly interpret subsurface structure. Of the two method proposed to correct topographic effect, the method incorporating topography explicitly in the inversion is applicable to wider range of survey data than the correction method since the latter requires some assumptions. For forward problem, it has been shown that the finite element method using unstructured tetrahedral element is useful to incorporate topography because it can represent complicated object precisely and robustly with relatively fewer elements. In this paper, using the newly developed code, the author shows the applicability of the unstructured tetrahedral element to MT inversion

The inversion code calculates electromagnetic field on the earth with the edge-based tetrahedral element. And it searches the subsurface resistivity and components of distortion matrix of each site as model parameters. In inversion, the code iteratively updates the models to minimize the object function consisting of the data misfit, the model roughness and the strength of galvanic distortion using the Gauss-Newton method. And, the code is parallelized with the OpenMP/MPI hybrid parallel programming.

The newly developed code was applied to synthetic data of the model including topography. As a result of the inversion, anomalies of true model were recovered correctly. This result showed that inversion using unstructured tetrahedral elements is useful to interpret resistivity structure correctly instead of topographic effect.

Resistivity imaging of source regions of Iwaki and N-Ibaraki normal faulting sequences

Makoto Uyeshima[1]; Yasuo Ogawa[2]; Masahiro Ichiki[3]; Weerachai Siripunvaraporn[4]
[1] ERI, Univ. Tokyo; [2] VFRC, Titech; [3] RCPEV, Grad. School of Sci, Tohoku Univ.; [4] Mahidol University, Thailand

Following the 2011 Tohoku-Oki earthquake, M9.0, several areas of the inland Japan were activated due to significant change of the stress field. Among all, intense swarm-like seismicity associated with shallow normal faulting was induced in Ibaraki and Fukushima prefectures in the boundary area between Kanto and Tohoku districts, Japan. In order to elucidate a structural model of electrical resistivity in this region and to get insights on causes of those induced earthquakes, MT surveys were performed in Jan. 2012 and from Dec., 2013 to Jan. 2014, by using Phoenix and Metronix wideband MT instruments.

We first estimated impedance tensors and induction vectors with the aid of the BIRRP code (Chave and Thomson, 2004) at the same sets of periods (from about 0.03s to 1000s) for both of the wideband MT instruments. We also combined the 3-D MT and induction-vector (IV) inversion code by Siripunvaraporn and Egbert, 2009 and the 3-D phase-tensor (PT) inversion code by Patro et al., 2013 to yield a 3-D PTIV inversion code. This modification aimed at finding a 3-D resistivity model free from influences of the static or galvanic effects.

We applied the PT-IV 3-D inversion code to the Iwaki and N-Ibaraki datasets. In order to investigate the influence of the initial model on the final structural model, we did several inversion runs with initial resistivity values ranging from 20 to 2000 Ohm-m. All the inversion runs could get respective final models with RMS of about 2. Although some differences in the final models are detected, overall characteristics and scales (in length and intensity) are similar for all the final models. Generally, induced earthquakes are distributed in the higher electrical resistivity zones. We delineated a separate low-resistivity anomaly directly beneath the hypocenter of the M7.0 Iwaki earthquake indicating crustal fluids in this region. Together with previously obtained seismic image (Kato et al., 2013), we hypothesize that strong crust underwent structural failure due to the infiltration of crustal fluids into the seismogenic zone from deeper levels, causing the Iwaki earthquake.

Resistivity structure around the 2011 earthquakes bellow Mt. Fuji volcano, Japan

Koki Aizawa[1]; Makoto Uyeshima[2]; Yusuke Yamaya[3]; Hideaki Hase[4]; Yasuo Ogawa[5]
[1] SEVO, Kyushu Univ.; [2] ERI, Univ. Tokyo; [3] GSJ, AIST; [4] KSVO, Tokyo Tech; [5] VFRC, Titech

On March 15 2011, 4 days after the Mw 9.0 megathrust Tohoku-Oki earthquake, the Mw 5.9 earthquake occurred beneath the southern flank of Mt. Fuji volcano. The aftershocks and the coseismic ground movement showed that the rupture is the left-lateral strike-slip with a strike of N24E at an approximate depth of 7˜13 km. Beneath the northern flank, the rate of micro-earthquakes increased gradually after the Tohoku earthquake. These earthquakes were on the approximately North-South trending line across the volcano, implying the earthquakes occurrence is guided by the structure. In this study, we show the electric resistivity structure around the focal zone of the earthquakes.

The MT data were obtained in the three campaigns. Between August and September 2009, audio-frequency band (10,000˜1 Hz) data was obtained to map the structure at shallow (˜3 km) level of the volcano. From June to December 2011, the broad-band (200˜0.001 Hz) MT data was obtained to elucidate the deep structure around the seismicity, then followed up by the observation in April-May 2012. Typical recording duration for one site is 1 night in the 2009 survey, and 3 weeks in the 2011-2012 surveys. In addition to these data, we also used the broad-band MT data recorded on 2002-2003 along the ENE-WSW line (Aizawa et al., 2004). By using these data, we estimated the resistivity structures by using the 2-D (Ogawa and Uchida, 1996) and 3-D inversion codes (Siripunvaraporn et al., 2009) on the assumption that the structure did not significantly change during 2002-2012. This assumption was confirmed by the comparison of the sounding curves of the sites where the MT data was recorded both in 2009 and 2011. The results show that the moderate (10˜100 ohm-m) conductive zone corresponds to the location of the seismicity, and suggest that the earthquakes occurred on the relatively fractured zone.

Acknowledgments

The geomagnetic data used for the remote-reference processing were provided by the Kakioka Geomagnetic Observatory, Japan Meteorological Agency. We thank landowners and regional forest offices (Shizuoka and Yamanashi prefectures) for permitting the observations to be conducted. A. Watanabe, K. Miyakawa, H. Abe, and TaWaT Rung-Arunwan, were thanked for field campaign. We thank W. Siripunvaraporn for supplying his 3-D inversion code. The 3-D inversion was conducted on the EIC of the Earthquake Research Institute, University of Tokyo. We thank to use of JMA seismic catalogue. This work was supported by a Grant-in-Aid from MEXT.

Definitive geomagnetic data at Yatsugatake geoelectromagnetic observatory in 2013

Tsutomu OGAWA[1]
[1] ERI, Univ. Tokyo

Yatsugatake geoelectromagnetic observatory (YAT) has been in operation as a reference station of the geomagnetic field for detecting and discussing tectonomagnetic and volcanomagnetic field variations. Definitive geomagnetic data at YAT in 2013 are obtained with baseline values determined by monthly absolute measurement, opened for the first time since the establishment of the observatory in 1970. Compared with the provisional data of which the baseline values are treated as constants, seasonal changes in the data which amounts to approximately 1minpp in the declination and 4nTpp in the vertical component are corrected in the definitive data. The definitive data show that the annual rates of the geomagnetic field change at YAT in 2013 are approximately -2min for the declination, -4nT for the horizontal component, +52nT for the vertical component and +37nT for the total intensity, respectively

ループループ法のための高精度三次元フォワード構造解析計算の検討

坂中 伸也 [1]; Selepeng Ame Thato[2]
[1] 秋田大・国際資源; [2] 秋田大・工学資源

Confirmation of precise numerical 3-D forward calculation of subsurface structure for loop-loop induction method

Shinya Sakanaka[1]; Ame Thato Selepeng[2]
[1] International Resource Sciences, Akita Univ.; [2] Engineering and Resource Science, Akita Univ.

The loop-loop induction method is one of electromagnetic exploration tools using a pair of transmitter and receiver coils for subsurface electrical structure. The loop-loop method is sometimes called as slingram method.

Although there are some kinds of manufacture instrument for the loop-loop method, we are now rather taking Geonics EM-34-3 into consideration. EM-34-3 has a pair of coils with 64 cm diameter and three lengths of coil separation cables, ie. 10 m, 20 m, 40 m. The exploration depth for the low induction number like as the loop-loop method is depending on the coil separation of transmitter and receiver. The exploration depths of EM-34-3 are from 7.5 m to 60 m for each length of separation and type of coil alignment.

Traditionally, the loop-loop method has been mainly used for reconnaissance survey and the 1-D analysis (McNeil, 1980) has been popularly adopted.

We sometimes faced on the negative apparent conductivity as observed value at high conductivity or high contrast of electrical structure areas. 1-D analysis of the loop-loop method is convenient but not able to apply to the negative apparent conductivity because 1-D electric structure never produces the negative apparent conductivity.

Now we focus on the theory of 3-D forward calculation introduced by Perez-Flores et al. (2012). They show the equations for apparent conductivity for types of coil alignments of VMD (vertical magnetic dipole) and HMD (horizontal magnetic dipole). The equations can calculated the apparent conductivity for complicated 3-D structure and can be used for even negative apparent conductivity. Perez-Flores et al. (2012) show some kinds of result for the structure models but we cannot know exact numerical calculation. We make consideration of pragmatic numerical calculation and find out succeeding method at present.

日本の地磁気変換関数長期変化の地域性

竹田 雅彦 [1]
[1] 京大・理・地磁気センター

Locality of geomagnetic transfer function in long-term variation in Japan

Masahiko Takeda[1]
[1] Data Analysis Center for Geomagnetism and Space Magnetism, Kyoto Univ.

Geomagnetic transfer function at several pbservatories in Japan was studied in the period of since 1985. Although most of the long-term variations are common at most observatories, and some of them are probably caused by the solar activity variation, different behavior of the variation was found at some observatories, which may be caused by time variation of the local conductivity structure in the earth.

日本の多くの観測所での地磁気変換関数の 1985 年以来の長期変化を調べた。外部場の変化の影響を小さくするため各日夜間 0h-4hLT のデータを用いて月別に計算し、それらの長期変化を算出した。その結果として長期的変化は概してほぼ全ての観測所に共通であり、それらには太陽活動度の変化を反映しているとみられるものも多いが、いくつかの観測所では特定の期間に特異的に変化しているケースも見出され、特に数分程度の短周期に顕著に見出された。これらは地球内部電気伝導度変化に起因する誘導電流の変化を反映している可能性があり、詳しくは学会時に報告する予定である。

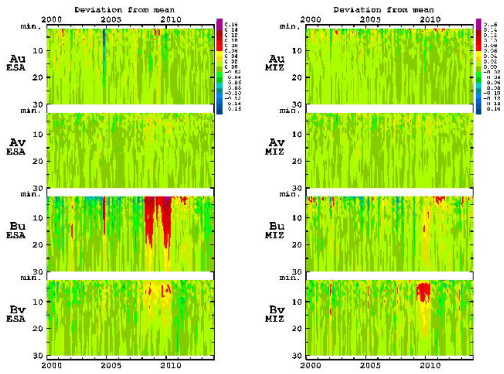

野島注水実験における自然電位変動モデル再構築

村上 英記 [1]
[1] 高知大・自然科学系・理学部門

Improved Line Source Model for self-potential variations during Nojima water injection experiments

Hideki Murakami[1]
[1] Natural Sciences Cluster-Science Unit, Kochi Univ.

Repeated water injection experiments have been done at the Nojima fault, which is responsible for the 1995 Hyogoken-nanbu earthquake (Mw6.9), to research the healing process of the fault. During experiments we have observed self-potential variations around a water injection borehole and estimated the time variation of hydraulic parameters around the fault. Observed self-potential variations during the experiments can be explained with streaming potentials due to the flow of the injected water. Negative anomalies of self-potential appear on the ground surface around the injection borehole because the change in self-potential in the aquifer is conducted to the whole part of the borehole through the iron pipe, which acts as a line source of electric current. However, during recent experiments positive changes of self-potential observed far away from the borehole. These changes are not well explained by the previous simple model. We must introduce the positive electric charges, which are ignored in the previous model, to explain the observations. We propose the improved model for self-potential variations associated with water injection experiments.

1995 年兵庫県南部地震（Mw6.9) の地表地震断層である野島断層の回復（固着）過程をモニターする目的で数年おきに注水実験が繰り返し実施されている。注水実験では，断層運動の直後は断層近傍が破砕された状態にあり水が流れやすい状態であり，時間経過とともに断層面の固着が進行し水は流れにくくなるという作業仮説の基に実施されている。これまでに，1997 年，2000 年，2003 年，2004 年，2006 年，2008 年，2013 年の計 7 回実施された。1997 年から 2008 年の実験では，当初の目論見とは異なり，断層破砕帯ではなく断層近傍の深さ 540m 付近から周囲への注水であったが，時間経過とともに水が通りにくくなっており地震発生後数年でほぼ定常状態になっていることが複数の観測から示唆されている（西上，2014)。

注水実験時に注水孔周辺の地表で自然電位の変動を観測し，地下の水の流動のしやすさの変化を観測してきた。1997 年から 2004 年までの実験では，注水時の自然電位変動として次の３つの特徴が観測された：１）注水の開始・停止に同期している，２）注水孔周辺が負に変動する，３）注水孔からの距離が大きくなると変動量が小さくなる。また，同レベルの流量・圧力に対する自然電位変動が年々大きくなるという現象も観測された。これらの自然電位の変動特性から，観測している自然電位変動は注水に伴う流動電位を観測しているものであり，地下の水理パラメータが年々小さくなっている，すなわち流れにくくなっているものと推定した（Murakami et al.,2001;Murakami et al.,2007)。

しかし，2006 年頃の実験からそれまでの自然電位変動とは異なる変動を示す観測点が出てきた（村上ほか，2010)。注水孔から離れた一部の地点での電位変動が，従来の注水に伴い負に変動するのではなく逆に正に変動するようになった。一方，注水孔の極近傍では従来通り注水の開始にともない負に変動している。また，いずれの観測点における自然電位変動は，注水の開始と停止に同期した変動であることにかわりはない。

これらの新たな変動は，従来の地下で発生した流動電位を注水孔のケーシングパイプが電流電極の役目を果たして地表に伝えるというモデルでは説明できない。従来の注水実験で観測された電位変動を説明するためには，水の流動方向が正になりケーシングパイプ側が負になるような電場が発生している必要がある。従来のモデルは，水の流れて行く方向の正の電荷の位置については無限遠とした近似モデルであった。正の電荷の位置を電位計測範囲に設定することで定性的に説明が可能になる。自然電位測定も含め複数の観測から水が流れにくくなっている，つまり水の流動範囲が注水孔の近くに限定されてきたということとも整合的である。発表においてはいくつかの定量的なモデルについて紹介する。

本研究の一部は，東京大学地震研究所平成 26 年度特定研究（A)「注水実験による内陸地震の震源断層の詳細な構造と回復過程の研究」から援助を受けておこないました。

FDTD 法を用いた地磁気誘導電場計算

木村 葵 [1]; 海老原 祐輔 [2]; 大村 善治 [3]; 菊池 崇 [4]
[1] 京大・生存圏・電気; [2] 京大生存圏; [3] 京大・生存圏; [4] 名大 STE 研

The calculation of geomagnetically induced electric field by using FDTD method

Aoi Kimura[1]; Yusuke Ebihara[2]; Yoshiharu Omura[3]; Takashi Kikuchi[4]
[1] RISH; [2] RISH, Kyoto Univ.; [3] RISH, Kyoto Univ.; [4] STEL, Nagoya Univ.

We have calculated geomagnetically induced electromagnetic field which is induced on the surface or underground by using frequency-domain analysis such as Fourier’s transform. It is surely valid for a horizontally equable ground structure, or it is not good for complex ground structure like Japan area. To calculate exact field, we have to use a method that can count a complex ground structure. In this time, we have FDTD to calculate geomagnetically induced electromagnetic field, and we get the distribution of electromagnetic field and current of grounds. In this result, we can observe how coast line effect occurs, and we can evaluate how conductivity, magnetic permeability contribute to the distribution of electromagnetic field and current.

HTS-SQUID磁力計を用いた高感度地磁気観測システムの評価

香取 勇太 [1]; 大久保 寛 [1]; 波頭 経裕 [2]; 田辺 圭一 [2]; 塚本 晃 [2]; 大西 信人 [3]; 古川 克 [3]; 磯上 慎二 [4]; 竹内 伸直 [5]
[1] 首都大東京・院・システデザ; [2] 超電導工研; [3] テラテクニカ; [4] 福島高専; [5] 東北大・院理・予知観測セ

An Evaluation of High Resolution Observation System Using HTS-SQUID Magnetometer

Yuta Katori[1]; Kan Okubo[1]; Tsunehiro Hato[2]; Keiichi TANABE[2]; Akira Tsukamoto[2]; Nobuhito Onishi[3]; Chikara Furukawa[3]; Shinji Isogami[4]; Nobunao Takeuchi[5]
[1] Graduate School of System Design, Tokyo Met. University; [2] ISTEC; [3] TIERRA TECNICA; [4] Fukushima National College of Technology; [5] Res Cent Predict Earthq Volcan, Tohoku Univ.

This study addresses the performance evaluation of high-resolution geomagnetic field observation system using HTS-SQUID (high-temperature-superconductor based super conducting quantum-interference-device) magnetometer.

By our past study, it was suggested that the geomagnetic variation signal accompanying fault movement, whose sources are the piezomagnetic effects, is very small, therefore development of a high-sensitive magnetometer system is very important.

Since March 2012, we have observed 3 components of the geomagnetic field using a HTS-SQUID magnetometer at Iwaki observation point in Fukushima, Japan.

In this study, we compare the signal observed by HTS-SQUID magnetometer with that of our flux-gate magnetometer at IWK and that of Kakioka Magnetic Observatory, and investigate the sensitivity and the resolution of the signal. Additionally, we show the geomagnetic signals observed during earthquake occurrences at Iwaki observation site.

本発表では、福島県いわき市において2012年3月より稼働しているHTS-SQUID磁力計を用いた高感度地磁気観測システムの評価を行った。

地震発生時における断層運動による震源付近の圧力変化が要因であるピエゾ磁気効果による磁場変化は非常に微小な信号であると考えられる。この信号を明確に観測し，検出するためには屋外での高感度磁力計による連続観測を行う必要がある。

本研究グループではHTS-SQUID磁力計を用いた観測を実施している。本発表では，いわき観測点において同時観測されたフラックスゲート磁力計の信号と比較解析し，本HTS-SQUID磁力計の野外観測時における感度を評価した結果を報告する。

東北地方太平洋沖地震に伴う磁場変動の解析

藤井 郁子 [1]; 歌田 久司 [2]; 平原 秀行 [3]; 仰木 淳平 [4]; 高橋 冬樹 [5]; 海東 恵美 [4]; 源 泰拓 [6]
[1] 気象大学校; [2] 東大・地震研; [3] 気象庁地磁気観測所; [4] なし; [5] 地磁気観測所; [6] 気象庁地磁気観測所

Geomagnetic field variations associated with the 2011 off the Pacific coast of Tohoku Earthquake

Ikuko Fujii[1]; Hisashi Utada[2]; Hideyuki Hirahara[3]; Jumpei Ogi[4]; Fuyuki Takahashi[5]; Megumi Kaito[4]; Yasuhiro Minamoto[6]
[1] Meteorological College; [2] ERI, Univ. Tokyo; [3] Kakioka,JMA; [4] none; [5] Kakioka Magnetic Observatory; [6] Kakioka Magnetic Observtory, JMA

Geomagnetic field variations observed at 19 sites from December, 2010 to April, 2011 were analyzed to investigate signals associated with the 2011 off the Pacific coast of Tohoku Earthquake that was occurred at 5:46 UT on March 11, 2011.

As a first step, we attempted to remove variations of main field and ionospheric/magnetospheric origin from the data which are uncorrelated to the earthquake. A procedure using a stochastic filter and one using a Kalman filter were tested resulting in large residual amplitudes at distant sites from a reference site. Log-term variations in the residual were relative to that of the reference data in the stochastic filter approach and that make it difficult to investigate a long-term variation associate with the earthquake.

The Empirical Orthogonal Function method (EOF, or also known as the Principal Component Method) was applied to the data set. Data gaps shorter than 30 minutes were temporally filled in the EOF analysis so that a larger portion of the data was analyzed. The time period used in the EOF analysis ranged from December 1, 2010 to March 11, 2011. Four (X, Y, Z and F) or two (X and Y) components were used.

Choices of the components or a small portion of the sites made no fundamental difference in the results. We briefly describe our results below.

No particular dominant modes were seen in the eigen values of the covariance matrix.

Spatial distributions of the first and second modes suggest that these are in-pahse variations in the Japan region. The third mode shows latitude dependency in the Y component except the Chichijima observatory. Higher modes are dominated by a few components. Therefore, variations whose spatial scales are smaller than the Japan region are scattered in the higher modes.

The residuals is computed by removing the first and second modes from the data.

No unusual variations are seen at first glance before the earthquake occurred. A trend variation just before the earthquake, which is claimed in GPS-TEC variations, is subtle.

Three vector components at Esashi changed at the same time as the earthquake, but no changes are seen at 19km-apart Mizusawa suggesting it is not of earthquake origin. The geomagnetic field at Kakioka slightly changed then, but effects of earthquake tremors might be remained according to the observation record at Kakioka.

The geomagnetic field at the eastern Japan started to slowly vary just after the earthquake. It might be difficult to detect a variation of mechanical origin out of this change, because Utada et al. (2011) and Zhang et al. (2014) showed the magnetic field changes when the tsunami occurred off shore.

The F component at Kakioka increased with unknown cause before the starting time of the GPS-TEC variation of tsunami origin.

The geomagnetic variations at most of the sites show variations at or after the starting time of the GPS-TEC variation of tsunami origin and those variations seem to be consistent with the GPS-TEC variation.

No substantial variations in the Z component are seen when the tsunami arrived at the sites of Honsyu island. That at Chichijima shows a clear periodic variation after 6:40 UT. A small variation caused by Tsunami induction may be seen in the F difference between Kakioka and Kitaura.

As a rough summary, pre- and coseismic changes are not substantial and the variation of Tsunami origin is detected.

2011 年 3 月 11 日 5:46UT に発生した東北地方太平洋沖地震に伴う変動を調べるため、2010 年 12 月～2011 年 4 月の全国 19 観測点の磁場 1 分値計 70 成分を解析した。

まずは、地震と無関係な電離圏・磁気圏起源の変動成分と主磁場成分を除去することを考える。確率差分法、カルマンフィルター法を試したが、参照点と観測点の距離が離れるにつれ残差が大きくなった。また、確率差分法では、残差のトレンドは相対的なものとなり、トレンドに反映されるような異常変動があったのかどうか解析できなくなる。

これらの問題を解消するため、Empirical Orthogonal Function 法（EOF 法あるいは主成分法）を適用することにした。30 分以内の欠測は AR フィルターで一時的にうめ、なるべく多くの観測値を解析できるようにした。解析期間は 2010 年 12 月 1 日から 3 月 11 日 7:15UT（北浦観測点停止時間）、あるいは 11 日 23：59UT（水沢観測点停止時間）となった。全成分を使った場合と XY 成分のみの場合の 2 種類の計算を行った。

北浦観測点の有無、ZF 成分の有無で、結果に根本的な差は見られなかった。以下に主要な結果を示す。

共分散行列固有値からは、とびぬけてパワーが強いモードがないことがわかった。

上位モードの空間分布を見ると、第 1 モードと第 2 モードが日本規模でほぼ一様に作用する広域変動となっている。第

3 モードは主に Y 成分の緯度依存性を示しているが、父島だけ値が小さくなっており、父島 Y 成分の寄与は第 4 モードに現れる。それ以上の高次モードは、少数の成分への寄与を中心としている。従って、地域的な変動や局所的な変動は高次モードに分散して取り込まれている。

1 分値から第 1 モードと第 2 モードを除去した残差を調べた。

2010 年 12 月から地震直前には、特に目を引く変化があるようには見えない。TEC で言われている本震発生前のトレンド変化も、あまり顕著ではない。

地震発生時には、江刺の 3 成分が 5:47 に変化しているが、19km 離れた水沢には見られず、地球物理的なシグナルではない可能性が高い。柿岡には発生直後にわずかなパルスが入っているが、地震直後のデータには地震動の影響が残っている可能性がある。

地震発生直後から、江刺や水沢で明瞭に、南は柿岡まで、ゆっくりとした変動が始まるのが見える。Utada et al. (2011) と Zhang et al. (2014) が、津波が沖合で発生した時、領域内の磁場が変動することを指摘していることを考慮すると、coseismic な力学現象起源の変化とみるのは難しいかもしれない。

地震発生直後から、TEC 変動発生時刻（5:53 ごろ）までの間に、柿岡 F には明瞭な正のピークがあり、北浦、大多喜でも見えるかもしれない。津波誘導磁場とは時刻と地理的分布がかみ合わないと思われ、原因は不明である。

TEC 変動発生時刻（5:53 ごろ）にほとんどの観測点でゆるやかな変動が始まり、その後、大きな変化が起こる。電離層震央からの距離に比例するように観測点を並べかえると、東北から離れる方向に伝播しているので、Tsugawa et al. (2011) が報告した TEC 擾乱が同心円状に広がっていくのを見ていると思われる。磁場変動は震源からの方角によって波形が異なっているが、これも TEC 擾乱と調和的である。

観測点に一番近い検潮所に津波実体波が到達した時刻付近の Z 成分の変動を目視で見た限りでは、本土の観測点では顕著な変化はない。父島では 6:40 くらいから明瞭な周期的変動が始まる。柿岡と北浦の F 成分の差を見ると、津波到達による変化がわずかに見えるかもしれない。

これらの特徴から、地震発生前の変化と地震と同時の変化では顕著なものは検出されず、発生直後に津波が作る磁場変動（津波誘導磁場と TEC 変動による磁場変化）は検出できていると思われる。